Cell cycle arrest in replicative senescence is not an immediate consequence of telomere dysfunction

M. Shamim Nassrally[a], Ashley Lau[a], Katherine Wise[a], Noah John[a], Sanjeev Kotecha[a], Kar Lai Lee[a], Robert F. Brooks[a,b,*]

[a] King's College London, Faculty of Life Sciences & Medicine, Department of Anatomy, Guy's Campus, LONDON SE1 1UL, UK
[b] St George's, University of London, Molecular and Clinical Sciences Research Institute, Mailpoint J2A, Cranmer Terrace, London, SW17 0RE, UK

ABSTRACT

In replicative senescence, cells with critically-short telomeres activate a DNA-damage response leading to cell-cycle arrest, while those without telomere dysfunction would be expected to cycle normally. However, population growth declines more gradually than such a simple binary switch between cycling and non-cycling states would predict. We show here that late-passage cultures of human fibroblasts are not a simple mixture of cycling and non-cycling cells. Rather, although some cells had short cycle times comparable to those of younger cells, others continued to divide but with greatly extended cycle times, indicating a more-gradual approach to permanent arrest. Remarkably, in late passage cells, the majority showed prominent DNA-damage foci positive for 53BP1, yet many continued to divide. Evidently, the DNA-damage-response elicited by critically-short telomeres is not initially strong enough for complete cell-cycle arrest. A similar continuation of the cell cycle in the face of an active DNA-damage response was also seen in cells treated with a low dose of doxorubicin sufficient to produce multiple 53BP1 foci in all nuclei. Cell cycle checkpoint engagement in response to DNA damage is thus weaker than generally supposed, explaining why an accumulation of dysfunctional telomeres is needed before marked cell cycle elongation or permanent arrest is achieved.

1. Introduction

Replicative senescence – a state of permanent cell cycle arrest following prolonged proliferation (Hayflick, 1965) – is due primarily to the erosion of telomeres, the specialized nucleotide repeat structures that protect the ends of linear eukaryotic chromosomes (Harley, 1991; Lundberg et al., 2000; Serrano and Blasco, 2001; Wright and Shay, 2001). Because DNA polymerases are unable to replicate fully the ends of linear DNA molecules, telomeric DNA shortens with each round of DNA replication (Harley, 1991). Germ cells (and some stem cells) express the enzyme telomerase which adds back multiple hexanucleotide repeats to compensate for this shortening (Hiyama and Hiyama, 2007; Wright et al., 1996). However, most somatic cells lack telomerase and can therefore undergo only a finite number of divisions before telomeres erode to the point where they resemble double-stranded DNA breaks, which evoke a DNA damage response leading to a loss of proliferative capacity and the cessation of culture growth (d'Adda di Fagagna et al., 2003; Rossiello et al., 2014). Telomere erosion can be prevented by ectopic expression of the telomerase reverse transcriptase catalytic subunit (TERT), which reconstitutes telomerase activity

(Colgin and Reddel, 1999). For human fibroblasts this is generally sufficient to prevent replicative senescence and "immortalize" the cells (Bodnar et al., 1998).

In its simplest form, the telomere-shortening hypothesis predicts a relatively abrupt loss of proliferative capacity towards the end of culture lifespan, as telomeres become critically short (Levy et al., 1992). However, it is well known that proliferative capacity is highly heterogeneous, even between sister cells, with non-dividing cells appearing from the earliest passage (Absher and Absher, 1976; Absher et al., 1974; Ponten et al., 1983; Smith and Whitney, 1980). To account for the heterogeneity, Blackburn suggested that stochastic telomere uncapping, rather than shortening per se, may be the critical event leading to the loss of proliferative capacity (Blackburn, 2000). It is also known that telomeric DNA is especially sensitive to oxidative damage which can thus accelerate the shortening (von Zglinicki et al., 1995; von Zglinicki et al., 2000). Moreover, even without significant shortening, damaged telomeres are resistant to repair in the absence of adequate telomerase activity, and accumulate in aging tissues (Fumagalli et al., 2012; Hewitt et al., 2012; Rossiello et al., 2014). Thus, random damage to telomeres, through exposure to reactive oxygen species (Passos et al., 2007), or

other stresses including stalled replication forks (Suram et al., 2012), could also contribute to the observed heterogeneity in proliferative capacity and the early appearance of senescent cells, even in the absence of detectable telomere shortening (Ferenac et al., 2005; Pitiyage et al., 2010; Victorelli and Passos, 2017).

The DNA-damage response elicited by critically short or damaged ("dysfunctional") telomeres results in the upregulation of p53, which in turn causes cell cycle arrest through the expression of p21 (CDKN1A), an inhibitor of the cyclin-dependent kinases (CDKs) needed for cell cycle initiation and mitosis (Brown et al., 1997; Wynford-Thomas, 2000). Nevertheless, although the link between dysfunctional telomeres and the DNA-damage response is well established, it remains unclear just how quickly permanent cell cycle arrest is achieved. Given the suggestion that just a single DNA double-strand break is sufficient for proliferative arrest (Di Leonardo et al., 1994), the onset of arrest at the cellular level in response to dysfunctional telomeres is widely regarded as an abrupt, all-or-none consequence of activating the DNA-damage response. In keeping with this, while the growth fraction drops progressively with passage, the cycle times of the few cells proliferating in late-passage cultures are reported to be identical to those of young cells (Bell et al., 1978; Karatza et al., 1984; Ponten et al., 1983), compatible with the idea that the onset of senescence is a binary switch between cycling and non-cycling states (Bell et al., 1978; Shall and Stein, 1979). However, others have reported that cycle times are elongated in late passage cultures (Macieira-Coelho et al., 1966) suggesting a more-gradual approach to proliferative arrest. Dysfunctional telomeres, positive for the DNA-damage marker γ-H2AX, have also been observed in metaphase spreads, indicating that cells with an active telomeric DNA-damage response must nevertheless be able to progress into mitosis (Kaul et al., 2011). On statistical grounds, it was estimated that the accumulation of 5 dysfunctional telomeres was necessary for irreversible cell cycle arrest (Kaul et al., 2011).

Further evidence in favour of a gradual approach to cell senescence has come from studies by Kim et al. (2013) which showed progressive changes in gene expression and various markers of cell senescence (e.g. increased cell size, area, and β-galactosidase staining) over many weeks after cell doubling time first began to increase. However, these studies were population-based so it was not possible to tell whether the increases in doubling times were due to decreases in growth fraction or a lengthening of the cell cycle, or both, while the changes in gene expression or cell senescence markers may have occurred in response to prolonged arrest, only in cells that had permanently left the cell cycle. The details of how and when permanent cell cycle arrest is reached are therefore important but remain to be established.

To clarify the kinetics of cell cycle arrest at the cellular level in response to telomere dysfunction, population-based methods of analysis such as BUdR labelling or flow cytometry are inadequate, as they give limited information about the variability and heterogeneity of cell cycle times within a population. Instead, direct measurements of cell cycle duration by time-lapse microscopy of individual cells are needed. Some such studies for human diploid fibroblasts have already been reported (Absher and Absher, 1976; Absher et al., 1974, 1975). However, the published data are for selected individual clones at different passage levels, and do not give the full measure of cell cycle variability and heterogeneity across a whole population. Furthermore, the cultures were not in steady state, making the cell cycle time distributions difficult to interpret (Shields, 1979; Smith, 1977). We have therefore undertaken further time-lapse studies of human diploid fibroblasts as they approach senescence and have compared the cycle time distributions to those of identical cells immortalized by telomerase. We find that clonal heterogeneity is not restricted to cells undergoing senescence but is also seen with immortalized cells. The variability of cell cycle times is substantial, even for immortalized cells, ranging from around 10 h to more than 90 h – much greater than commonly realized. In late-passage cultures of normal fibroblasts, some cells continue to divide with cycle times similar to those of earlier passage or

immortalized cells. However, others divide only after greatly extended cycle times suggesting that the onset of growth arrest in senescence is not a simple, irreversible binary switch between cycling and non-cycling states but involves a more gradual slow-down in proliferation. Of particular note, we find that many late passage cells continue to cycle despite the presence of prominent telomere-related DNA-damage foci. This suggests that the initial DNA-damage response evoked by dysfunctional telomeres is not sufficient for immediate, permanent arrest. This is not because DNA-damage signalling from dysfunctional telomeres is ineffective in some way since we find that cells treated with a low dose of doxorubicin also continue to cycle while showing an active, DNA-damage response. Rather, cell cycle checkpoint engagement in response to DNA damage is weaker than generally supposed. This explains why an accumulation of dysfunctional telomeres, through continued cycling, is needed before marked cell cycle elongation or permanent arrest is achieved.

2. Materials and methods

2.1. Cell culture

Hs68 neonatal foreskin fibroblasts (ATCC: CRL 1635) and dermal fibroblasts from a 24 year old male homozygous for a 19 bp deletion in exon 2 of the *CDKN2A* gene (Leiden cells), together with their TERT-immortalized counterparts (Brookes et al., 2002) were kindly provided by Gordon Peters (CRUK, London). In Leiden cells, the *CDKN2A* deletion specifically eliminates p16^{Ink4a} function while retaining a fully functional ARF (Brookes et al., 2002). The cells were grown routinely at 37 °C and 8% CO_2 in Dulbecco's modified Eagle's medium (DMEM) containing 25 mM glucose, 1 mM sodium pyruvate and 10% foetal calf serum (FCS), hereafter referred to as growth medium. In most cases, the cells were cultured in 25 cm^2 tissue culture flasks (Nunc) with 7 ml of growth medium and an initial seeding density of 0.5×10^5 cells/flask. However, for the Hs68 growth curves in Fig. 1, the cells were grown in 80 cm^2 tissue culture flasks (Nunc) with 14 ml of growth medium, and an initial seeding density of 2.5×10^5 cells/flask. The cells were subcultured at weekly intervals for the most part, with a medium-change on day 3 or 4. For subculture, the cells were detached using 0.05% (w/v) trypsin (GIBCO) in Dulbecco's phosphate buffered saline solution A (PBS$_A$) containing 0.02% (w/v) EDTA, counted using a haemocytometer, and the number of population doublings achieved in that passage calculated. As the normal fibroblast cultures neared the end of their life-span, the interval required to reach confluence (and subculture) increased. They were considered to have reached their terminal passage when cell number failed to double over an interval of 4 weeks, with twice-weekly medium changes. Because lifespan (maximum number of population doublings achieved) varied slightly with different batches of FCS, in order to compare experiments over time, cell growth was expressed as a fraction of the completed lifespan.

2.2. β-Galactosidase staining

Cells were rinsed twice with PBS$_A$, fixed with 2% formaldehyde/ 0.2% glutaraldehyde in PBS$_A$ and stained for senescence-associated (SA) β-galactosidase (at pH 6.0), as described (Dimri et al., 1995).

2.3. Time-lapse films

For time-lapse microscopy, 2×10^3 cells were seeded in a 0.1 ml drop of growth medium in the centre of a 25 cm^2 flask. After incubation at 37 °C for at least 30 min to allow the cells to attach, the flasks were flooded with 7 ml of growth medium and returned to the incubator to equilibrate. The local cell density achieved was comparable to the seeding density in routine subculture, but the total number of cells in the flask was far less (only 2%), in order to minimise medium depletion during the course of a film. For filming, the flask was transferred to a
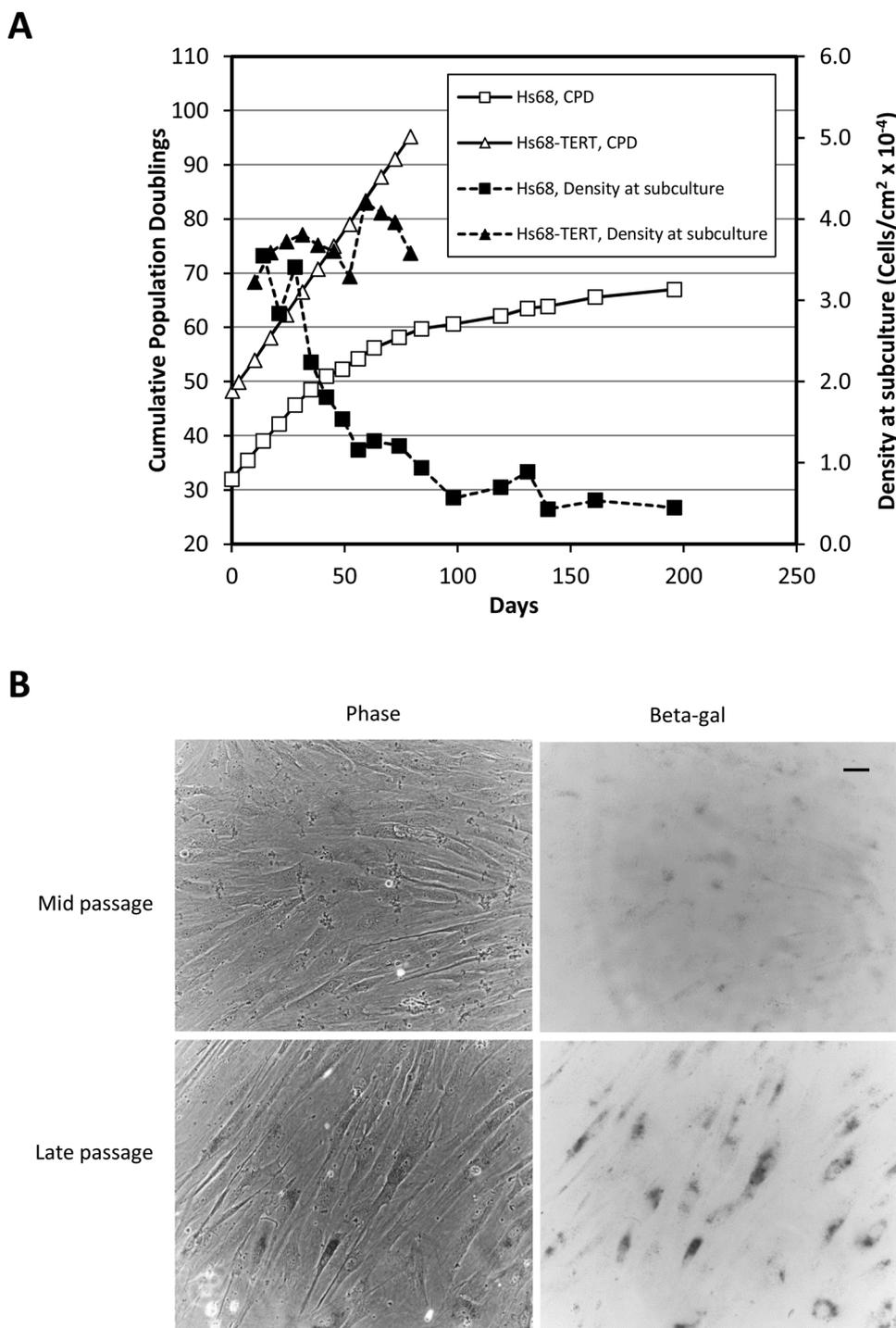
A

B

Fig. 1. Growth characteristics of Hs68 and Hs68-TERT cells.
(A) Population growth curves and cell density at subculture (confluence) for normal Hs68 cells and their TERT-immortalized counterparts (CPD, cumulative population doublings).
(B) Hs68 cells stained for senescence-associated (SA) beta galactosidase at mid-passage (corresponding to 34 population doublings in A) or late passage (corresponding to 62 population doublings in A). Right-hand panels, bright field, showing SA beta-galactosidase; left-hand panels, corresponding phase contrast images. Scale bar = 20 μm.

Zeiss inverted microscope fitted with a heated stage set to achieve a temperature of 37 °C within the flask. The flask was covered with a clear Pyrex "hot plate", which had a heating element painted on to it (Riddle, 1983) and maintained at a temperature slightly above 37 °C, to prevent the build-up of mist on the top surface of the flask. The flask was surrounded by an expanded polystyrene jacket cut to fit around it, and covered by a clear Perspex box placed over it on top of the stage as an insulator, to help keep the temperature of the flask constant. Filming was started 1–3 days after plating, to ensure the cells had resumed exponential growth following subculture. Images were captured using a monochrome video camera and Panasonic time-lapse video recorder at one frame per minute, or later with a Moticam digital camera, at 15 min intervals.

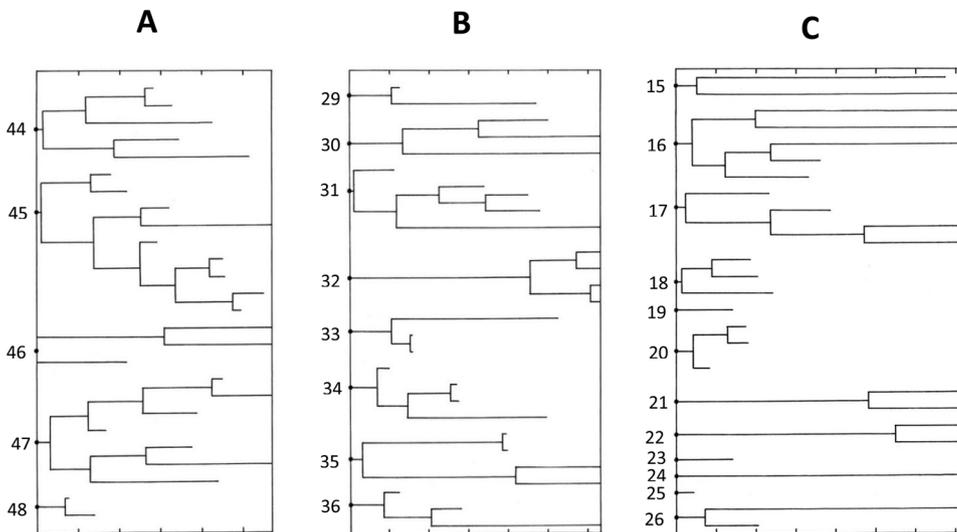Using the films, individual cells were tracked until they divided,

A　　　　**B**　　　　**C**

died or were lost from view. Dead cells or cells dividing abnormally were noted but discarded from the analysis of division times. Cells lost to view were included in the analysis up to the point they were lost, as described (Smith, 1977).

2.4. Immunofluorescence staining for 53BP1

Cells were seeded into 3 cm dishes (Nunc) at 2×10^4 per dish in 2 ml of medium (DMEM plus 10% FCS), and used 4–5 days later. After first rinsing with PBS_A (DIFCO), the cells were fixed with methanol at −20 °C for 5 min, and air-dried. Using an inverted 0.5 ml microfuge tube as a template, a grease circle was painted around the cells in the centre of the dish using a cotton bud dipped in petroleum jelly. Cells within the circle were then rehydrated with PBS_A containing 1% bovine serum albumin (BSA) for 5 min., and incubated overnight at 4 °C with 20 μl of rabbit anti-53BP1 (Cell Signalling Technology, Cat. 4937) diluted 1:100 in PBS_A containing 1% BSA and 0.15% sodium azide. After removing the primary antibody, the cells were rinsed x3 with PBS_A before staining with 20 μl of AlexaFluor 488-conjugated goat anti-rabbit IgG (H + L) from Molecular Probes (Life Technologies, Cat. A-11008), diluted 1:100 in PBS_A containing 1% BSA and 0.15% sodium azide, for 60 min at 37 °C. Following removal of the secondary antibody, the cells were rinsed x3 with PBS_A, then stained for DNA with 4′,6′-diamidino-2-phenylindone (DAPI) at 1 μg/ml in PBS_A for 5 min, and finally covered with a 22 mm coverslip mounted using Fluorosave (Calbiochem). The cells were then examined using an Olympus PROVIS AX70 microscope. Fluorescence images were captured using a Zeiss Axiocam digital camera using the AxioVision software.

3. Results

3.1. Progressive decline in cell density at confluence prior to senescence

The growth characteristics of the Hs68 fibroblasts used in this study are shown in Fig. 1. They typically reached 60–70 population doublings (Fig. 1A), before entering a state of stable growth arrest in which the cells were positive for "senescence-associated" β-galactosidase (Fig. 1B).

For the growth curves in Fig. 1A, the cells were subcultured shortly after the attainment of confluence, in late-logarithmic growth. The cell density attained is therefore close to saturation and delaying subculture would make little difference to the number of cells harvested. It is noteworthy that the cell density at confluence dropped progressively with passage, long before the slow-down in population growth associated with senescence became apparent. This decline in cell density

was invariable over many similar experiments, and indicates an early increase in average cell area during progression to senescence, as reported by Kim et al. (2013). It was also seen with fibroblasts ("Leiden cells") derived from an individual bearing inactivating mutations in both alleles of the p16^{Ink4A} (CDKN2 A) gene (Supplementary Fig. S1) and is not therefore dependent on the expression of p16, the Cdk4/6 inhibitor implicated in telomere-independent senescence in some cell types (Serrano and Blasco, 2001). Rather, the decline is an early manifestation of telomere dysfunction since it is not seen when the cells are immortalized with TERT (Fig. 1A and Fig. S1). If the transition between cycling and non-cycling states in senescence were abrupt, a decline in cell density at confluence would not be expected until near the end of culture lifespan, since the small, not-yet-senescent cycling cells should continue to proliferate unhindered, filling up the culture surface. However, we do not see nests of small, cycling cells interspersed amongst large, non-cycling (senescent) cells (Fig. 1B). Rather, the steady decline in saturation density with passage suggests a more-gradual transition to cell-cycle arrest than a simple switch might predict.

3.2. Late passage cells continue cycling with extended cycle times

3.2.1. Time-lapse analysis

In its simplest form, the telomere dysfunction hypothesis of replicative senescence predicts a binary switch from a proliferative to a non-proliferative state such that cells with critically short or damaged telomeres undergo arrest while the rest continue to cycle normally (Blackburn, 2000). To determine if this was the case, given the rather gradual decline in saturation density over time in Fig. 1, late passage Hs68 cells were followed by time-lapse microscopy and their cell-cycle behaviour compared with that of mid-passage cells, or cells immortalized with TERT. Typical cell pedigrees for one such representative experiment are shown in Fig. 2A–C. The full set of pedigrees is given in supplementary Fig. S2A–C, and the complete listing of cell division times in Tables S1A-C. Details of how the cell division times are codified are indicated in Fig. S3.

Many TERT-immortalized cells could be followed through three consecutive divisions (two complete cell cycles) or more (Fig. 2A; Supplementary Fig. S2A). In contrast, the late-passage cells (85% of completed lifespan, corresponding to 58 population doublings in Fig. 1A) underwent far fewer consecutive cell cycles in a similar interval (Fig. 2C; Supplementary Fig. S2C), some cells failing to divide at all and others only after extended cell cycle times (e.g. cells 21 and 22). The late-passage cells (being flatter) were also much harder to follow, identity often becoming ambiguous after collisions with adjacent cells. As a result, many more cells were marked as "lost". The mid-passage

Hs68 cells (64% of completed lifespan, corresponding to 44 population doublings in Fig. 1A) showed intermediate behaviour compared to the late-passage cells and TERT-immortalized cells (Fig. 2B; Supplementary Fig. S2B).

Clonal heterogeneity has long been recognized as a feature of normal diploid cells (Absher and Absher, 1976; Absher et al., 1974; Ponten et al., 1983; Smith and Whitney, 1980) and is clearly evident here. For example, cell 32 (mid-passage cells, Fig. 2B) does not divide until 90.5 h after the start of the film. This is more than 9 times the minimum cycle time for these cells (9.75 h) and a point when other cells have undergone up to four consecutive divisions (e.g. cell 31, Fig. 2B). However, such heterogeneity is also seen with TERT-immortalized cells. For example, cell 46 (Fig. 2A) divides at the very start of the film. One of its daughters is subsequently lost but the other does not divide again until after 61.5 h, a point when adjacent cells have completed up to three consecutive cycles (e.g. cells 45 and 47, Fig. 2A). Heterogeneity in TERT-immortalized cells is also observed *within* clones. For example, cell 13 (Supplementary Fig. S2A) divides 4.5 h after the start of the film. One of its daughters does not divide again until after a further 95 h, while its sibling completes two further cell cycles in the same interval. Heterogeneity in proliferative capacity is clearly not restricted to cells undergoing replicative senescence.

3.2.2. Distribution of times to first mitosis after the start of filming

The kinetics of entry into mitosis are shown in Fig. 3A. For the TERT-immortalized cells, roughly 96% of the 60 cells followed reached mitosis during the 114.5 h of the film (Fig. 3A), the longest recorded time to first mitosis being 59.75 h (cell 11, Fig. S2A). Two cells were followed for longer than this without dividing but were lost before the end of the film (cells 20 and 21, Fig. S2A). Considering that the cells are growing at their maximal rate, under optimal conditions, the range of times to first division (0 to > 59.75 h) is very large, indicating a degree of cell cycle variability that is rarely appreciated.

For the mid-passage cells (64% completed lifespan) and late-passage cells (85% completed lifespan), the initial rate of entry into mitosis appears lower than for the TERT-immortalized cells (Fig. 3A). This is most likely due to differences in the degree of synchrony following replating of the cells which affects the proportion already in S or G_2 at the start of the film. The rate of entry into the cell cycle is better assessed by considering the cohort of cells dividing after the minimum cycle time for these cells (9.75 h, in this case). This cohort corresponds roughly to the cells in G_1 not yet committed to the next cycle at the start of the film. (Cells dividing in the initial segment of the film up to the minimum cycle time would be mainly those already in S or G_2 at the start of the film.) As seen in Fig. 3B, the initial rate of entry into mitosis for this "G_1 cohort" is essentially identical for all three cultures. For the mid-passage and TERT immortalized cells, the rates are similar over the entire film, though with a possible slight excess of very long cycle times in the mid-passage cells. However, for the late-passage cells, there is a marked slow-down in entry into mitosis after the first 30% of the cohort divides, indicating a reduced probability of cell cycle initiation. The longest recorded division time was 116.75 h (cell 35 in Supplementary Fig. S2C), roughly 12 times greater than the minimum cycle time for these cells (9.75 h); 9 other cells were followed to the end of the film (145 h) without dividing.

Apart from the cell cycle slow-down seen with the late-passage cells, it is also noteworthy that 5 of the 55 cells tracked died without dividing, during the course of the film (Supplementary Fig. S2C). In contrast, no cell death was observed prior to the first mitosis in the films of mid-passage or immortalized cells (Supplementary Fig. S2A, B).

The data in Fig. 3A might suggest a decrease in growth fraction with passage, as reported by others (Cristofalo and Sharf, 1973; Karatza et al., 1984; Ponten et al., 1983). Thus, only 69% of the late passage cells divided at least once during the 6 days (145 h) of the film, compared to 96% with the immortalized TERT cells. Nevertheless, it cannot be concluded that all of the cells remaining undivided at the end of the
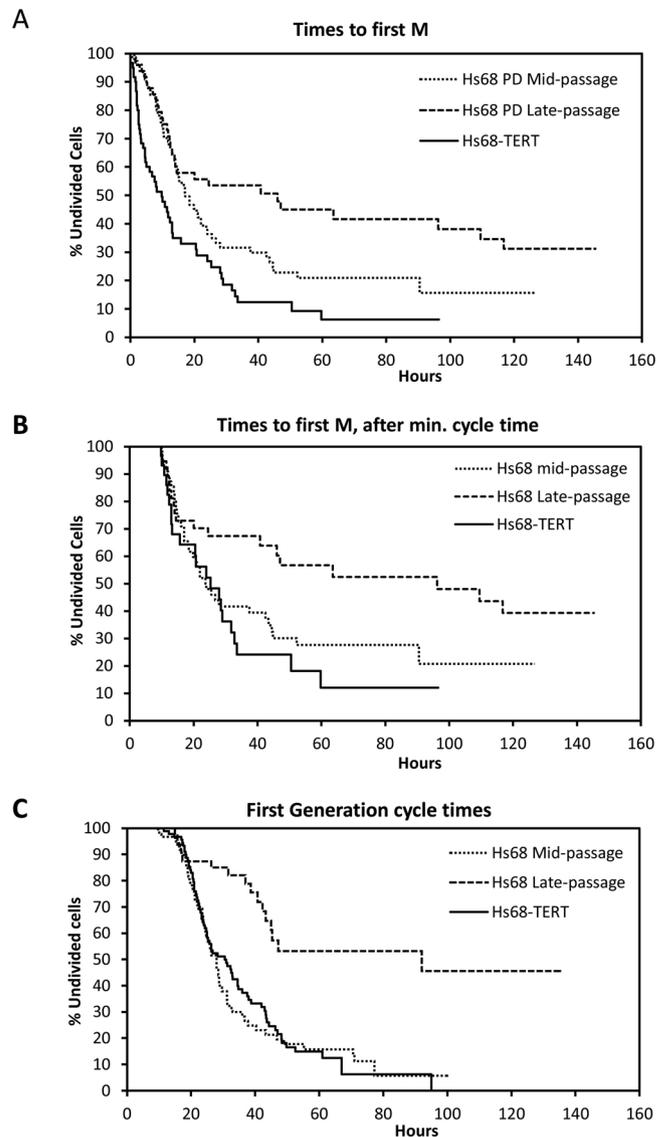

Fig. 3. Cell division times for late- and mid-passage Hs68 fibroblasts and their TERT-immortalised counterparts. The data are derived from the full set of cell pedigrees in Supplementary Fig. S2, for immortalized Hs68-TERT fibroblasts, and normal Hs68 cells at mid passage (64% completed lifespan) or late passage (85% completed lifespan). Lost cells were included in the analysis up to the point they were lost, as described (Smith, 1977).

(A) Times to first mitosis after the start of filming. For the late passage cells, the number of cells followed was 55, of which 6 died during the period of observation (145 h). For the mid-passage cells and TERT cells, the initial sample sizes were 76 and 60 respectively, with no cell death observed. After ranking, the times to division were plotted as the fraction of cells not yet divided against time.

(B) Times to first mitosis for cells dividing 9.75 h (the minimum cycle time in this experiment) *after* the start of filming, roughly corresponding to the cohort of cells in G1 at the beginning of the film. The initial sample sizes were 29 (TERT cells), 55 (mid-passage) and 37 (late-passage). Data plotted as in (A).

(C) First generation cycle times. The daughters of cells dividing in panel A were followed until they in turn divided, died or were lost from view. After ranking, the interdivision times were plotted as the fraction of cells not yet divided against cell age (hours). For the late passage cells, the number of cells that could be followed was 51, of which 3 died without dividing before the end of the film. For the mid-passage cells and TERT cells, the numbers of cells that could be followed were 89 and 92 respectively, with no cell death noted.
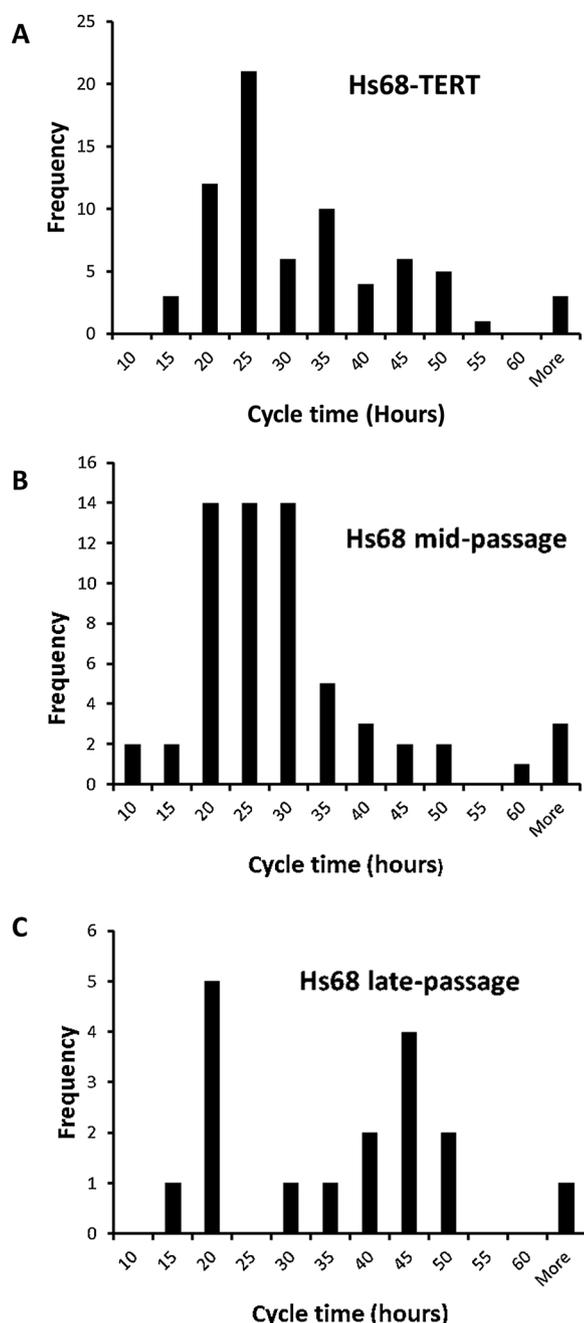
Fig. 4. First generation cycle time distributions (complete interdivision times only).
(A) immortalized Hs68-TERT fibroblasts; (B) normal Hs68 cells at mid passage (64% completed lifespan); (C) normal Hs68 cells at late passage (85% completed lifespan). The sample sizes were 71, 62 and 17 respectively. The data are from the full set of cell pedigrees in Supplementary Fig. S2.

film were permanently incapable of further division since many of them may have reached mitosis had the period of observation been even longer. Indeed, this seems likely, since the plot of undivided cells against time does not plateau in the late passage culture but continues to fall throughout the period of observation, albeit at a very low rate. What is certain is that the late passage culture shows an increase in the proportion of cells dividing with extremely long cycle times, compared to the mid-passage culture.

3.2.3. Cycle times

The progeny of the cells dividing were followed until they in turn

divided or were lost to view, in order to determine complete cell cycle duration. The resulting first generation cycle times are shown as "alpha curves" (Kaplan–Meier plots) (Brooks et al., 1980; Smith and Martin, 1973) in Fig. 3C or as frequency histograms (complete cycle times only) in Fig. 4. The distributions of cycle times for the mid-passage cells (64% completed lifespan) and the TERT-immortalized cells were virtually identical (Figs. 3C; 4 A,B) with a growth fraction of essentially 100%, indicating that the mid-passage cells which divide generate progeny that remain highly proliferative. In contrast, for the late passage cells (85% completed lifespan), only 54% of the cells divided for a second time (i.e. one complete cell cycle) during the period of observation (Fig. 3C). The first of those to reach the second mitosis (around 15% of the cohort) had cycle times comparable to the shortest in the mid-passage and TERT cells (note the initial overlap in the alpha plots in Fig. 3C), but thereafter there was a shift towards longer cycle times (Figs. 3C; 4 C). Thus, in the late passage culture, although some cells still cycled as rapidly as TERT-immortalized cells, others did so with extended cycle times, as found for times to first mitosis (Fig. 3A). What is not found is a simple bifurcation between rapidly-dividing and non-dividing (growth-arrested) states.

3.3. Late passage cells show DNA damage foci yet continue to divide

To determine the association between full growth arrest, cell cycle elongation and the telomere-dysfunction-induced DNA-damage response, cells were stained with an antibody to 53BP1, a well-established marker of DNA-damage (d'Adda di Fagagna et al., 2003). Examples of nuclei with one, two and three prominent 53BP1-positive foci are shown in Fig. 5. For late-passage cells (84% completed lifespan), the fraction of positive cells was high, with 80% of the cells having at least one 53BP1-focus, and 20% having 3 or more (Fig. 6A). In contrast, only 15% of TERT-immortalized cells were positive (Fig. 6A), the majority of these having a single focus that was generally smaller than those seen in the non-immortalized cells (bottom row, Fig.5). The few, small foci seen in the TERT-cells are most likely a measure of "spontaneous" (random) DNA damage due (for example) to oxidative stress or incomplete replication (Arora et al., 2017; Barr et al., 2017). However, it has also been shown (Lee et al., 2015) that telomere extension in telomerase-expressing cells requires ATM-kinase function (usually co-localized with 53BP1 – d'Adda di Fagagna et al., 2003), raising the possibility that a transient DNA-damage response is a normal part of telomerase-dependent telomere maintenance. But regardless of the origin of the few small foci in TERT-immortalized cells, it seems clear that the majority of the (much larger) foci found in the non-immortalized cells are a consequence of telomere dysfunction since they are not seen in cells expressing telomerase.

In a parallel culture followed by time-lapse microscopy, 58% of the cells present in the field of view divided at least once over a 200 h period (Fig. 6B), comparable to the late-passage cells in Fig. 3. However, only 20% of the cells had no 53BP1-foci (Fig. 6A). Assuming, conservatively, that all these 53BP1-negative cells were among those that divided, it follows that the remaining 38% of cells (i.e. 58% minus 20%) that divided must have done so despite the presence of one or more prominent DNA-damage foci. Clearly, the presence of telomere-related DNA-damage foci does not identify the subpopulation of arrested, non-cycling cells. The DNA-damage response evoked by dysfunctional telomeres is evidently not always strong enough to bring about immediate, permanent cell cycle arrest.

Similar results were obtained with p16-null Leiden fibroblasts. The fraction of 53BP1-positive cells increased steadily with subculture, reaching 93% in late passage cells (87% completed lifespan, Fig. 6C). As with Hs68 cells, the majority of these 53BP1 foci must have been associated with telomere dysfunction since only around 9% of immortalized Leiden-TERT cells had any such foci in this experiment (Fig. 6C). In a comparable late-passage culture followed by time-lapse microscopy, 46% of the cells entered mitosis and divided over the 200 h
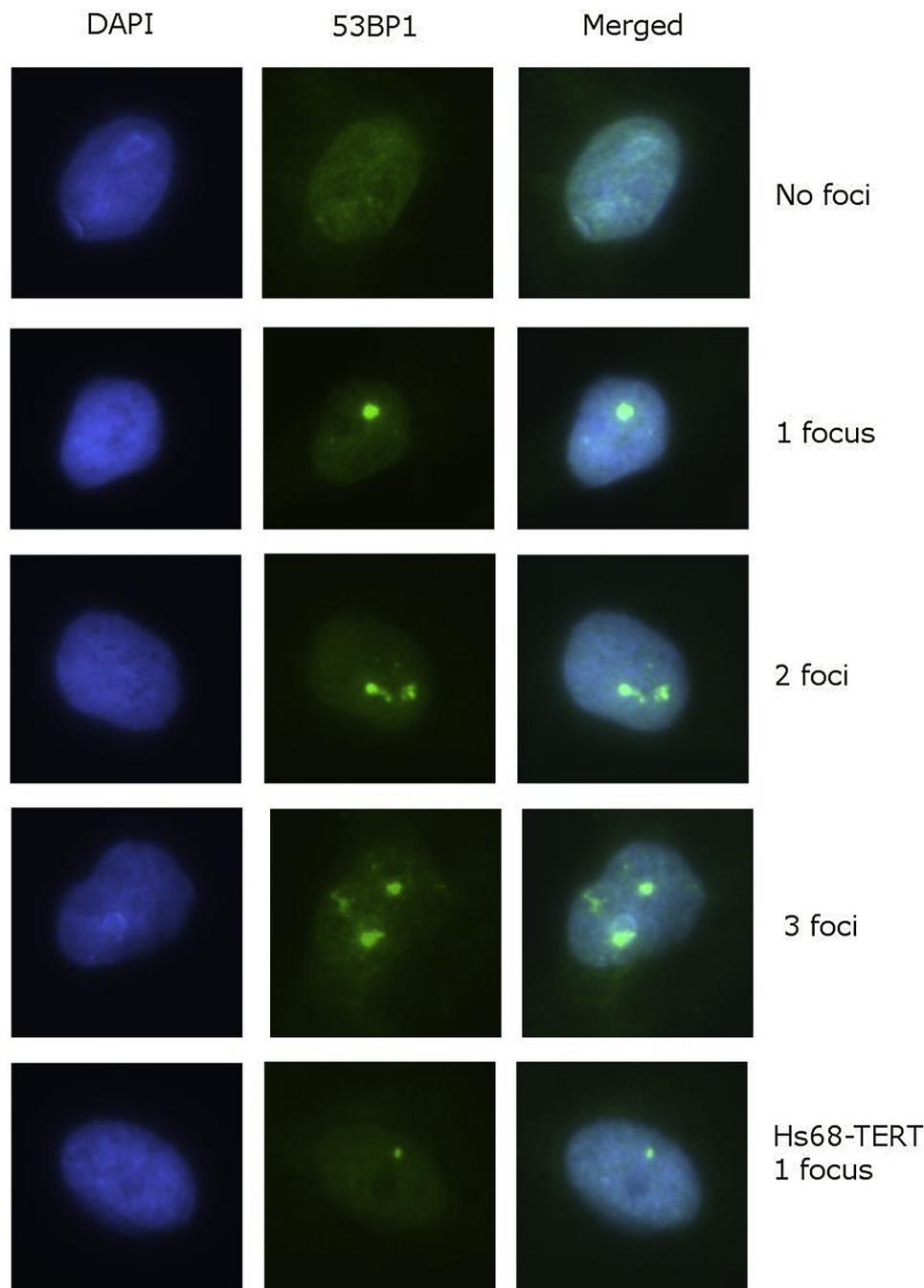
Fig. 5. Examples of DNA-damage foci (53BP1-positive) in moderately late passage normal Hs68 cells or immortalized Hs68-TERT cells. Rows 1–4 show examples of nuclei with 0, 1, 2 and 3 prominent 53BP1-positive foci (Hs68 cells), disregarding minor speckles. With immortalized Hs68-TERT cells, only small 53BP1-positive foci were observed. Row 5 shows an example of one such focus.

period of observation (Fig. 6D). Since 93% of the population was positive for 53BP1 foci, the majority of these dividing cells must have done so in spite of an active DNA-damage response.

Assuming that the 54% of cells remaining undivided at the end of the film were permanently arrested, this fraction was subtracted to give the times to mitosis of the dividing fraction (Fig. 6D). As with late passage Hs68 cells (Figs. 3 and 4), the dividing cells had extended cycle times compared to their TERT-immortalized counterparts (Fig. 6D). In this case, since these cells lack p16, it can be concluded that this cell cycle elongation does not depend on p16 expression.

The continued entry into mitosis of late-passage cells in spite of a telomere-related DNA-damage response raised the possibility that *progress* through mitosis might nevertheless be perturbed, due for example

to centrosome amplification or end-to-end chromosome fusions (Smogorzewska and de Lange, 2002). To examine this, the duration of mitosis (from rounding up to the onset of cytokinesis) was compared for late-passage cells (both Hs68 and Leiden cells) and their TERT-immortalized counterparts (Fig. 7A, B). For most cells, the duration of mitosis was between 45–60 min. However, for the late-passage cultures (both Hs68 and Leiden fibroblasts) there was a significant increase in the number of cells undergoing a prolonged mitosis (> 75 min). Some of these appeared to be multipolar mitoses, though in all cases here these resolved (after a delay) to give two viable daughters, sometimes of unequal size. In a few cases, daughter cells remained connected by a thin cytoplasmic process for an extended interval, suggestive of possible anaphase bridges. It thus seems likely that entry into mitosis by cells
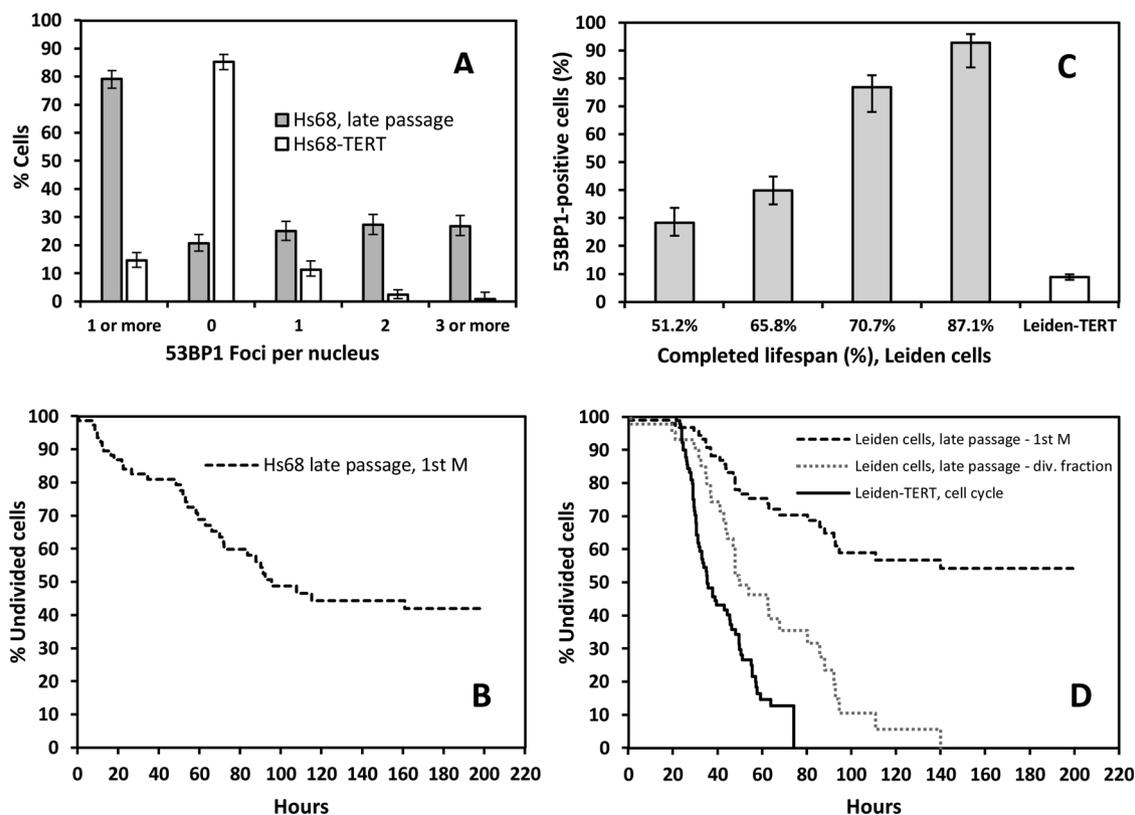
Fig. 6. Continued entry into mitosis in late passage Hs68 and Leiden cells showing telomere-related DNA-damage foci.
(A) Frequency of DNA-damage foci (53BP1-positive) per nucleus in late passage normal Hs68 cells (84% completed lifespan; shaded bars), and immortalized Hs68-TERT cells (open bars), with the 95% confidence intervals as indicated. (B) Times to first mitosis for late passage Hs68 cells (comparable to those in panel A). Filming commenced 3 days after plating the cells. (C) The frequency of 53BP1-positive Leiden cells increases with passage (% completed lifespan; shaded bars). Also shown is the frequency of 53BP1-positive Leiden-TERT cells (open bar). The error bars indicate the 95% confidence intervals. (D) Times to first mitosis for late passage Leiden cells (comparable to the highest passage in panel C). Filming was started 24 h after plating and in this experiment there was a further lag of around 20 h before cell division resumed. Also shown are the times to mitosis for the dividing fraction after subtraction of the non-dividing subpopulation (those still undivided at the end of the film), together with the distribution of intermitotic times for the immortalized Leiden-TERT cells under the same conditions.

with telomere dysfunction is not without consequence, consistent with the high frequency of abnormal nuclei (morphology, size, ploidy) commonly seen in senescent cultures, e.g. Sherwood et al. (1988); Smogorzewska and de Lange (2002).

3.4. Cells with DNA-damage induced by doxorubicin also continue to enter mitosis

The continued division of cells with telomere-related DNA-damage foci (Fig. 6B, D) was surprising and raised the possibility that the DNA-damage response evoked by dysfunctional telomeres might be incomplete in some way and activate cell cycle arrest more weakly than DNA breaks elsewhere in the genome. To examine this, TERT-immortalized Hs68 cells were treated with 0.2 μM doxorubicin for 1 h. This induces a strong DNA-damage response (multiple 53BP1 foci) in 100% of the cells (Fig. 8A), which persists for many hours. Indeed, even after 24 h, more than 80% of the cells continue to show one or more 53BP1 foci (not shown). Two hours after doxorubicin removal, to allow time for induction of downstream DNA-damage signalling, filming of the cells was commenced. Remarkably, from the start of filming, the cells continued to divide at much the same rate as untreated cells (Fig. 8B). Although some attempts at division were abnormal (prolonged rounding up, multipolar mitosis, failure of cytokinesis), as marked by the closed diamonds (♦) in Fig. 8B, it is clear that there was no early block to entry into mitosis. Of the cells followed, only around 20% underwent a prolonged cell cycle arrest (no division for up to 100 h). When this non-dividing cohort is subtracted, the times to mitosis for the dividing fraction were superimposable on the control over

the entire range (not shown). Thus, despite substantial DNA damage in all cells (Fig. 8A), 80% of the cells continued through the cell cycle with little if any delay.

To determine the subsequent fate of the doxorubicin-treated cells that divided, their daughters were followed through the next cell cycle. Almost 60% of these were observed to divide again during the course of the film, though with somewhat elongated cycle times compared to the control cells (Fig. 8B, inset). Thus, although the doxorubicin-treated cells showed little perturbation in the first cell cycle, there was some delay in the subsequent cycle, comparable to the extended cycle times seen in late passage cells (Figs. 3, 4, 6D). There is therefore little reason to suppose that DNA damage induced by doxorubicin produces a stronger activation of cell cycle checkpoints than does telomere dysfunction. Note however that when growing cells were re-plated and then exposed continuously to doxorubicin (after re-attachment), in contrast to the 1-hour treatment above, there was virtually complete suppression of cell division (not shown), confirming that Hs68 cells are fully capable of growth arrest in response to sufficient DNA damage.

4. Discussion

The telomere-dysfunction hypothesis of replicative senescence leads to an expectation that late-passage cultures should consist of a mixture of arrested cells (displaying an active, telomere-related DNA damage response) and cells cycling normally that have not yet acquired dysfunctional telomeres – given that telomere length is known to be heterogeneous both within and between cells of the same population (Allsopp and Harley, 1995; Levy et al., 1992). This, in turn, is supported
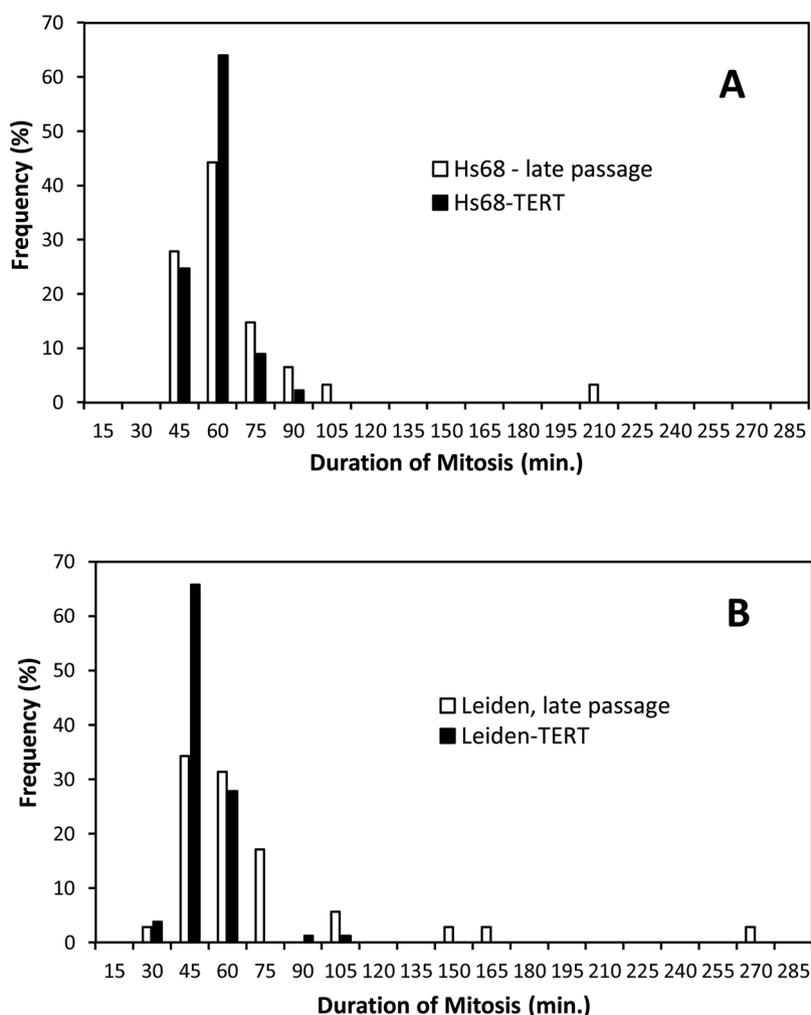
Fig. 7. Duration of mitosis in late-passage Hs68 and Leiden cells in comparison to their TERT-immortalized counterparts. Duration of mitosis for (A) the dividing late-passage Hs68 cells in Fig. 6B, and (B) the dividing late-passage Leiden cells in Fig. 6D, together with that for their TERT-immortalised counterparts under the same conditions. For both (A) and (B), the difference between the two distributions (wild type vs. TERT-immortalised) is significant (Chi square, $p < 0.05$). In the time-lapse films used, images were captured at 15 min intervals. The duration of mitosis was taken from rounding up to the onset of cytokinesis.

by reports that the few dividing cells present in high-passage cultures have cycle times identical to those of "young" cells (Bell et al., 1978; Karatza et al., 1984; Ponten et al., 1983). However, such a binary switch between cycling and non-cycling states predicts a relatively abrupt approach to culture senescence as telomeres shorten (Levy et al., 1992), which we do not see. Rather, with Hs68 fibroblasts (Fig. 1), and p16-null Leiden fibroblasts (Fig S1), cell density at confluence drops progressively long before the terminal passage, suggesting a more-gradual approach to cell senescence. This is consistent with the early increase in cell area at confluence reported by Kim et al. (2013).

In order to explore the onset of cell cycle arrest and senescence at the cellular level, we have undertaken time-lapse studies of cells approaching senescence. We find that while some late-passage cells do indeed continue cycling with cycle times comparable to young cells, others divide only after greatly extended cycle times. This indicates a slowing of the cell cycle rather than complete arrest, confirming that the loss of proliferative capacity is acquired gradually and is not an abrupt, all-or-none transition. Moreover, since similar results were seen with both Hs68 neonatal foreskin fibroblasts (Figs. 3 and 4) and Leiden cells (p16-null adult skin fibroblasts) (Fig. 6D), this slowing of the cell cycle is likely to be a general feature of cells approaching replicative senescence and one that does not require the induction of p16.

To determine the relationship between cell cycle elongation/arrest and telomere dysfunction, cells were stained for the DNA-damage

marker, 53BP1. As expected, the proportion of cells positive for 53BP1 foci rose steadily with passage (Fig. 6C), though not in cells expressing TERT, confirming that most, if not all, of the prominent foci are associated with telomere dysfunction. However, surprisingly, at a point where 80% of Hs68 cells had at least one, prominent 53BP1 focus per nucleus (Fig. 6A), 58% of the cells were seen to divide, by time-lapse microscopy, over a 200 h period of observation (Fig. 6B). Assuming that the 20% of cells without foci were among the dividers, it follows that 38% of the cells must have continued to enter and complete mitosis despite the presence of an active DNA-damage response. Similarly, 46% of late-passage Leiden fibroblasts divided successfully (Fig. 6D) even though 93% of the cells were positive for 53BP1 foci (Fig. 6C). Clearly, the presence of 53BP1 foci does not identify a sub-population of non-cycling cells, though it most likely accounts for the elongated cycle times shown by many of the late passage cells that continue to divide. Presumably, those with the longest cycle times and those that failed to divide at all during the 200 h of observation, are the cells with the greatest number of DNA damage foci. However, further work will be required to confirm this.

The continued division of cells with telomere-related DNA-damage foci raises the question as to whether the damage is repairable or irreparable. Given their much lower frequency in TERT-immortalized cells, most of the large 53BP1 foci seen here in normal late passage Hs68 and Leiden fibroblasts (Fig. 5) are likely to be associated with
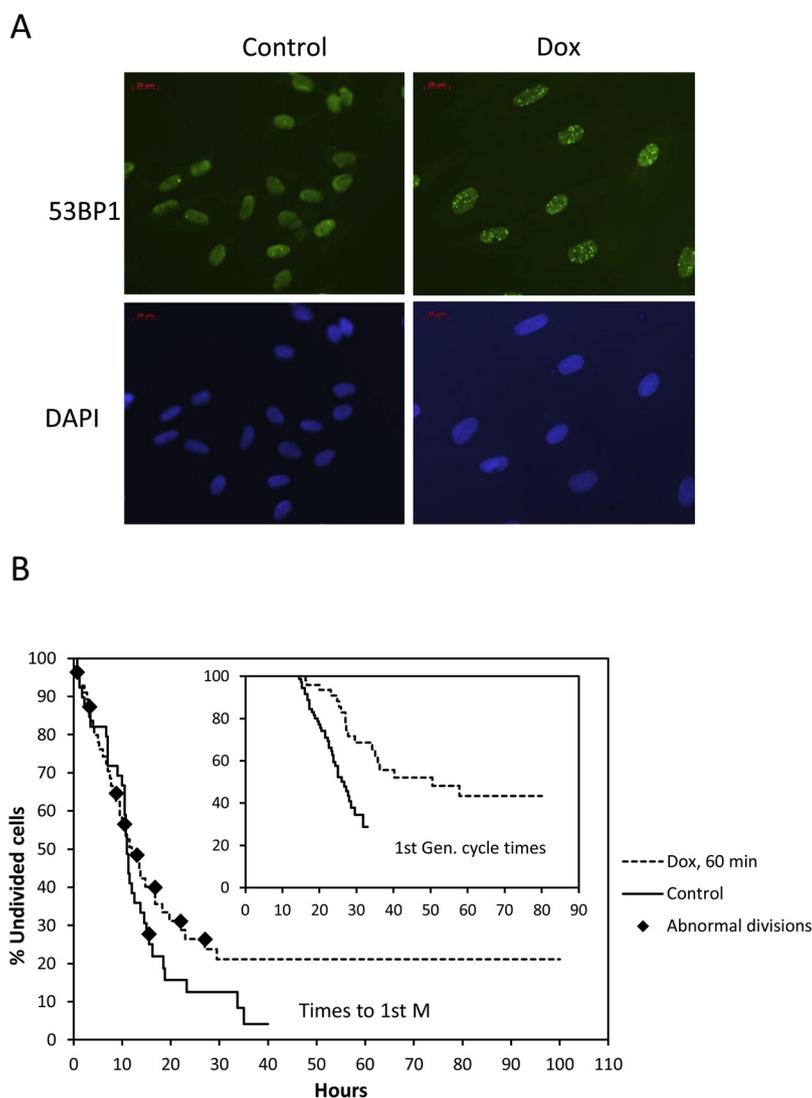
A

B

telomere "uncapping" (unravelling of the T-loop and exposure of a DNA end) caused by replication-driven telomere shortening (Price, 2012), though co-staining for telomeres by fluorescence in situ hybridization (FISH) is formally required to confirm this. With sufficient shortening, the uncapping is thought to become irreversible, leading to a persistent DNA-damage response to the chromosome end as a "break". However, in the early stages, there may be some degree of recapping (telomere "flip-flop" - Price, 2012; Blackburn, 2000) which could temporarily interrupt the DNA-damage response, allowing the cell cycle to resume. It is also possible that some large 53BP1 foci are associated with double-strand breaks *within* the telomere, rather than an exposed end (Victorelli and Passos, 2017). In rapidly proliferating cells, such telomere damage can be repaired by homologous recombination (Doksani and de Lange, 2016; Mao et al., 2016), though not in senescent cells (Mao et al., 2016). Any such repair prior to full senescence could again interrupt the DNA-damage response allowing the cell cycle to resume. Lastly, in senescent cells, some 53BP1 foci are not associated with telomeres but with DNA breaks elsewhere in the genome caused by increased levels of reactive oxygen species (ROS) (Passos et al., 2010). Such foci are transient as a result of DNA repair. Thus, it cannot be assumed that all of the 53BP1 foci seen here in late passage cells are permanent. Is it possible therefore that the cells that divide are ones that temporarily lose all their foci? We think not. The very high frequency of positive cells (> 90%, in Fig. 6C), maintained over time (and indeed rising with passage), means that any foci that disappear must be

rapidly replaced by new foci, and it is difficult to see how any cells could be without all foci for the length of time needed to complete a cell cycle. It therefore seems inescapable that some late passage cells are continuing to cycle in the presence of an active DNA-damage response. Nevertheless, live-cell imaging of cells expressing a GFP-tagged 53BP1 (Passos et al., 2010) is needed to confirm this.

Another explanation for how cells with telomere-related DNA-damage foci can continue to divide is that downstream signalling from dysfunctional telomeres is impaired compared to DNA breaks elsewhere in the genome, perhaps due to the suppression of DNA repair by telomere-associated proteins (Fumagalli et al., 2012; Hewitt et al., 2012; Rossiello et al., 2014). However, cells treated for a short time with a low dose of doxorubicin (sufficient to induce multiple DNA-damage foci in 100% of the cells) also continued to reach mitosis with comparatively little perturbation, though with some delay in the next cell cycle compared to control cells not treated with doxorubicin (Fig. 8). Although surprising, this is in accord with other recent reports that cells with *endogenous* DNA damage are able to pass through mitosis, but with delay in the subsequent cell cycle (Arora et al., 2017; Barr et al., 2017; Harrigan et al., 2011; Koundrioukoff et al., 2013; Lukas et al., 2011; Moreno et al., 2016). In particular, cells with 53BP1 foci were able to continue through G_1 for resolution in S phase. From all this, there is no reason to think that non-telomeric DNA damage evokes a stronger block to the cell cycle than does telomere dysfunction. Rather, cell cycle checkpoint engagement following DNA damage is evidently weaker

than generally supposed, and only when the damage is substantial is prolonged arrest in G_1 likely. Nevertheless, many of the studies quoted above (including those in Fig. 8) employed immortalized cells, so some caution may be called for in extrapolation to fully normal, non-immortalized cells in general.

Our results help to explain reports that an average of 5 dysfunctional telomeres is needed for permanent cell cycle arrest (Kaul et al., 2011). Thus, it seems likely that the first critically short or damaged telomere is not enough to arrest the cell cycle, enabling the cell to go through further rounds of replication, permitting further telomere erosion or damage. Presumably, only after the accumulation of at least 5 dysfunctional telomeres is the level of p53 and p21 induction sufficient for complete cell cycle arrest. Nevertheless, the late passage cells still contained some cells in S phase (Kaul et al., 2011). Rather than total arrest, a continued low rate of entry into S phase leading to further telomere shortening and eventual chromosome fusion could explain both the increased cell death rate and the increased duration of mitosis in some cells observed here in late passage cultures, as well as the increase in polyploidy and chromosome aberrations noted by others in senescence (Sherwood et al., 1988; Smogorzewska and de Lange, 2002). The presence of unrepaired DNA-damage in late-passage cells could also sensitize them to apoptosis during subculture, accounting for the reduced plating efficiency of cells approaching senescence shown by many strains of human fibroblasts, including those used here (unpublished). In addition, continued attempts to cycle in the face of unrepaired DNA-damage could account for the reduced viability seen in some fibroblast strains (e.g. WI-38 and IMR90) at very late passage, leading to the selective loss of cells with the highest extent of DNA-damage over time (Fumagalli et al., 2014).

The cell pedigrees shown in Figs. 2 and S2 illustrate the extent of cell cycle variability in populations of human fibroblasts growing rapidly and as they approach senescence. Even for TERT-immortalised cells under optimal conditions, the cell cycle times range from a minimum of around 10 h to more than 90 h (Fig. 3C), and there are many examples of proliferative heterogeneity both between and within clones (Fig. S2A), as previously reported for immortal mouse 3T3 cells (Brooks and Riddle, 1988a). Such heterogeneity is clearly not a distinguishing characteristic of cells undergoing senescence. One important consequence of this is that attempts to assess growth arrest in senescence by labelling with BUdR or [³H]-thymidine for intervals of 24 h (e.g. Fumagalli et al., 2014) or even 72 h (e.g. Dimri et al., 1995), are wholly inadequate to establish permanent cell cycle exit, given that some immortalized cells have cycle times that are longer than this, in cultures growing optimally.

The causes of cell cycle variability have been the subject of extensive debate over the years. According to one view, the variability is an intrinsic feature of the cell cycle resulting from the probabilistic, switch-like activation of one or two rate-limiting transitions (Smith and Martin, 1973; Brooks et al., 1980). Although the identity of the hypothetical transitions has never been established, recent plausible candidates include an RB-E2F bistable switch (Lee et al., 2010), abrupt degradation of the CDK2 inhibitor p27^{kip1} (CDKN1B) (Barr et al., 2016), or switch-like irreversible inactivation of APC^{CDH1}, the ubiquitin ligase whose targets include SKP2 needed for degradation of p21 and p27^{kip1} (Cappell et al., 2016). However, transition probability models do not readily account for the inter- and intra-clonal proliferative heterogeneity that becomes more extreme under limiting growth factor stimulation (Brooks and Riddle, 1988b). More recently, live-cell imaging of cells with fluorescent markers of cell cycle position has suggested that the transition between cycling and quiescent (G_0-like) states can be governed by the level of p21 in the mother cell at the time of mitosis and inherited by the daughter cells, and that this in turn is determined by endogenous DNA damage (or incomplete replication) in the mother cell (Arora et al., 2017; Barr et al., 2017; Overton et al., 2014; Spencer et al., 2013; Yang et al., 2017). Such endogenous DNA damage inherited from the previous cycle could well account for the limited

clonal heterogeneity seen here in TERT-immortalized fibroblasts while the added response to dysfunctional telomeres could explain the increased heterogeneity and extended cycle times seen in late passage normal fibroblasts lacking telomerase. Nevertheless, the fraction of TERT cells with DNA damage foci is generally less than 20%. If this fraction is assumed to correspond to the cells with the longest cycle times, the remaining 80% of the cells still have cycle times ranging from roughly 10–45 hours (Fig. 3C). Thus, a substantial fraction of the total cell cycle variability must be caused by something other than the response to DNA damage, such as the stochastic transitions postulated by transition probability models (Smith and Martin, 1973; Brooks et al., 1980).

Lastly, it is worth noting that the increasing frequency of dysfunctional telomeres with passage would lead to increasing basal levels of p21 in the population which would negatively compete with mitogen signalling in regulating entry into S phase though inhibition of CDK4/cyclin D (Yang et al., 2017). Thus, as levels of p21 rise, the cells would increasingly resemble cells starved of growth factors. Given the relationship between saturation density and serum growth factor concentration (Holley and Kiernan, 1968), this could provide an explanation for the progressive fall in saturation density with passage, as seen here (Fig. 1).

Declarations of interest

None

Funding

Appendix A. Supplementary data

Supplementary data associated with this article can be found, in the online version, at https://doi.org/10.1016/j.mad.2019.01.009.

References

Absher, P.M., Absher, R.G., 1976. Clonal variation and aging of diploid fibroblasts. Cinematographic studies of cell pedigrees. Exp. Cell Res. 103, 247–255.

Absher, P.M., Absher, R.G., Barnes, W.D., 1974. Genealogies of clones of diploid fibroblasts. Cinematographic observations of cell division patterns in relation to population aging. Exp. Cell Res. 88, 95–104.

Absher, P.M., Absher, R.G., Barnes, W.D., 1975. Time-lapse cinemicrophotographic studies of cell division patterns of human diploid fibroblasts (WI-38) during their in vitro lifespan. Adv. Exp. Med. Biol. 53, 91–105.

Allsopp, R.C., Harley, C.B., 1995. Evidence for a critical telomere length in senescent human fibroblasts. Exp. Cell Res. 219, 130–136.

Arora, M., Moser, J., Phadke, H., Basha, A.A., Spencer, S.L., 2017. Endogenous replication stress in mother cells leads to quiescence of daughter cells. Cell Rep. 19, 1351–1364.

Barr, A.R., Heldt, F.S., Zhang, T., Bakal, C., Novák, B., 2016. A dynamical framework for the all-or-none G1/S transition. Cell Syst. 2, 27–37.

Barr, A.R., Cooper, S., Heldt, F.S., Butera, F., Stoy, H., Mansfeld, J., Novák, B., Bakal, C., 2017. DNA damage during S-phase mediates the proliferation-quiescence decision in the subsequent G1 via p21 expression. Nat. Commun. 8, 14728. https://doi.org/10.1038/ncomms14728.

Bell, E., Marek, L.F., Levinstone, D.S., Merrill, C., Sher, S., Young, I.T., Eden, M., 1978. Loss of division potential in vitro: aging or differentiation? Science 202, 1158–1163.

Blackburn, E.H., 2000. Telomere states and cell fates. Nature 408, 53–56.

Bodnar, A.G., Ouellette, M., Frolkis, M., Holt, S.E., Chiu, C.P., Morin, G.B., Harley, C.B., Shay, J.W., Lichtsteiner, S., Wright, W., 1998. Extension of life-span by introduction of telomerase into normal human cells. Science 279, 349–352.

Brookes, S., Rowe, J., Ruas, M., Llanos, S., Clark, P.A., Lomax, M., James, M.C., Vatcheva, R., Bates, S., Vousden, K.H., Parry, D., Gruis, N., Smit, N., Bergman, W., Peters, G., 2002. INK4a-deficient human diploid fibroblasts are resistant to RAS-induced senescence. EMBO J. 21, 2936–2945.

Brooks, R.F., Riddle, P.N., 1988a. Differences in growth factor sensitivity between individual 3T3 cells arise at high frequency: possible relevance to cell senescence. Exp. Cell Res. 174, 378–387.

Brooks, R.F., Riddle, P.N., 1988b. The 3T3 cell cycle at low proliferation rates. J. Cell. Sci. 90, 601–612.

Brooks, R.F., Bennett, D.C., Smith, J.A., 1980. Mammalian cell cycles need two random transitions. Cell 19, 493–504.

Brown, J.P., Wei, W., Sedivy, J.M., 1997. Bypass of senescence after disruption of p21$^{CIP1/WAF1}$ gene in normal diploid human fibroblasts. Science 277, 831–834.

Cappell, S.D., Chung, M., Jaimovich, A., Spencer, S.L., Meyer, T., 2016. Irreversible APCCdh1 inactivation underlies the point of no return for cell-cycle entry. Cell 166, 167–180.

Colgin, L.M., Reddel, R.R., 1999. Telomere maintenance mechanisms and cellular immortalization. Curr. Opin. Genet. Dev. 9, 97–103.

Cristofalo, V.J., Sharf, B.B., 1973. Cellular senescence and DNA synthesis. Thymidine incorporation as a measure of population age in human diploid cells. Exp. Cell Res. 76, 419–427.

d'Adda di Fagagna, F., Reaper, P.M., Clay-Farrace, L., Fiegler, H., Carr, P., von Zglinicki, T., Saretzki, G., Carter, N.P., Jackson, S.P., 2003. A DNA damage checkpoint response in telomere-initiated senescence. Nature 426, 194–198.

Di Leonardo, A., Linke, S.P., Clarkin, K., Wahl, G.M., 1994. DNA damage triggers a prolonged p53-dependent G1 arrest and long-term induction of Cip1 in normal human fibroblasts. Genes Dev. 8, 2540–2551.

Dimri, G.P., Lee, X., Basile, G., Acosta, M., Scott, G., Roskelley, C., Medrano, E.E., Linskens, M., Rubelj, I., Pereira-Smith, O., Peacocke, M., Campisi, J., 1995. A biomarker that identifies senescent human cells in culture and in aging skin in vivo. Proc. Natl. Acad. Sci. 92, 9363–9367.

Doksani, Y., de Lange, T., 2016. Telomere-internal double-strand breaks are repaired by homologous recombination and PARP1/Lig3-dependent end-joining. Cell Rep. 17, 1646–1656.

Ferenac, M., Polančec, D., Huzak, M., Pereira-Smith, O.M., Rubelj, I., 2005. Early-senescing human skin fibroblasts do not demonstrate accelerated telomere shortening. J. Gerontol.: Series A 60, 820–829.

Fumagalli, M., Rossiello, F., Clerici, M., Barozzi, S., Cittaro, D., Kaplunov, J.M., Bucci, G., Dobreva, M., Matti, V., Beausejour, C.M., Herbig, U., Longhese, M.P., d'Adda di Fagagna, F., 2012. Telomeric DNA damage is irreparable and causes persistent DNA-damage-response activation. Nat. Cell Biol. 14, 355–365.

Fumagalli, M., Rossiello, F., Mondello, C., d'Adda di Fagagna, F., 2014. Stable cellular senescence is associated with persistent DDR activation. PLoS One 9, e110969.

Harley, C.B., 1991. Telomere loss: mitotic clock or genetic time bomb? Mutat. Res. 256, 271–282.

Harrigan, J.A., Belotserkovskaya, R., Coates, J., Dimitrova, D.S., Polo, S.E., Bradshaw, C.R., Fraser, P., Jackson, S.P., 2011. Replication stress induces 53BP1-containing OPT domains in G1 cells. J. Cell Biol. 193, 97–108.

Hayflick, L., 1965. The limited in vitro lifetime of human diploid cell strains. Exp. Cell Res. 37, 614–636.

Hewitt, G., Jurk, D., Marques, F.D.M., Correia-Melo, C., Hardy, T., Gackowska, A., Anderson, R., Taschuk, M., Mann, J., Passos, J.F., 2012. Telomeres are favoured targets of a persistent DNA damage response in ageing and stress-induced senescence. Nat. Commun. 3, 708. https://doi.org/10.1038/ncomms1708.

Hiyama, E., Hiyama, K., 2007. Telomere and telomerase in stem cells. Br. J. Cancer 96, 1020–1024.

Holley, R.W., Kiernan, J.A., 1968. "Contact inhibition" of cell division in 3T3 cells. Proc. Natl. Acad. Sci. U. S. A. 60, 300–304.

Karatza, C., Stein, W.D., Shall, S., 1984. Kinetics of in vitro ageing of mouse embryo fibroblasts. J. Cell. Sci. 65, 163–175.

Kaul, Z., Cesare, A.J., Huschtscha, L.I., Neumann, A.A., Reddel, R.R., 2011. Five dysfunctional telomeres predict onset of senescence in human cells. EMBO Rep. 13, 52–59.

Kim, Y.M., Byun, H.O., Jee, B.A., Cho, H., Seo, Y.H., Kim, Y.S., Park, M.H., Chung, H.Y., Woo, H.G., Yoon, G., 2013. Implications of time-series gene expression profiles of replicative senescence. Aging Cell 12, 622–634.

Koundrioukoff, S., Carignon, S., Técher, H., Letessier, A., Brison, O., Debatisse, M., 2013. Stepwise activation of the ATR signaling pathway upon increasing replication stress impacts fragile site integrity. PLoS Genet. 9, e1003643.

Lee, T.J., Yao, G., Bennett, D.C., Nevins, J.R., You, L., 2010. Stochastic E2F activation and reconciliation of phenomenological cell-cycle models. PLoS Biol. 8, e1000488.

Lee, S.S., Bohrson, C., Pike, A.M., Wheelan, S.J., Greider, C.W., 2015. ATM kinase is required for Telomere elongation in mouse and human cells. Cell Rep. 13, 1623–1632.

Levy, M.Z., Allsopp, R.C., Futcher, A.B., Greider, C.W., Harley, C.B., 1992. Telomere end-replication problem and cell aging. J. Mol. Biol. 225, 951–960.

Lukas, C., Savic, V., Bekker-Jensen, S., Doil, C., Neumann, B., Sølvhøj Pedersen, R., Grøfte, M., Chan, K.L., Hickson, I.D., Bartek, J., Lukas, J., 2011. 53BP1 nuclear bodies form around DNA lesions generated by mitotic transmission of chromosomes under replication stress. Nat. Cell Biol. 13, 243–253.

Lundberg, A.S., Hahn, W.C., Gupta, P., Weinberg, R.A., 2000. Genes involved in senescence and immortalization. Curr. Opin. Cell Biol. 12, 705–709.

Macieira-Coelho, A., Ponten, J., Philipson, L., 1966. The division cycle and RNA-synthesis in diploid human cells at different passage levels in vitro. Exp. Cell Res. 42, 673–684.

Mao, P., Liu, J., Zhang, Z., Zhang, H., Liu, H., Gao, S., Rong, Y.S., Zhao, Y., 2016. Homologous recombination-dependent repair of telomeric DSBs in proliferating human cells. Nat. Commun. 7, 12154. https://doi.org/10.1038/ncomms12154.

Moreno, A., Carrington, J.T., Albergante, L., Al Mamun, M., Haagensen, E.J., Komseli, E.S., Gorgoulis, V.G., Newman, T.J., Blow, J.J., 2016. Unreplicated DNA remaining from unperturbed S phases passes through mitosis for resolution in daughter cells. Proc. Natl. Acad. Sci. 113, E5757–E5764.

Overton, K.W., Spencer, S.L., Noderer, W.L., Meyer, T., Wang, C.L., 2014. Basal p21 controls population heterogeneity in cycling and quiescent cell cycle states. Proc. Natl. Acad. Sci. 111, E4386–E4393.

Passos, J.F., Saretzki, G., Ahmed, S., Nelson, G., Richter, T., Peters, H., Wappler, I., Birket, M.J., Harold, G., Schaeuble, K., Birch-Machin, M.A., Kirkwood, T.B.L., von Zglinicki, T., 2007. Mitochondrial dysfunction accounts for the stochastic heterogeneity in telomere-dependent senescence. PLoS Biol. 5, e110.

Passos, J.F., Nelson, G., Wang, C., Richter, T., Simillion, C., Procter, C.J., Miwa, S., Olijslagers, S., Hallinan, J., Wipat, A., Saretzki, G., Rudolph, K.L., Kirkwood, T.B.L., von Zglinicki, T., 2010. Feedback between p21 and reactive oxygen production is necessary for cell senescence. Mol. Syst. Biol. 6, 347. https://doi.org/10.1038/msb.2010.5.

Pitiyage, G.N., Slijepcevic, P., Gabrani, A., Chianea, Y.G., Lim, K.P., Prime, S.S., Tilakaratne, W.M., Fortune, F., Parkinson, E.K., 2010. Senescent mesenchymal cells accumulate in human fibrosis by a telomere-independent mechanism and ameliorate fibrosis through matrix metalloproteinases. J. Pathol. 223, 604–617.

Ponten, J., Stein, W.D., Shall, S., 1983. A quantitative analysis of the aging of human glial cells in culture. J. Cell. Physiol. 117, 342–352.

Price, C.M., 2012. Telomere flip-flop: an unfolding passage to senescence. EMBO Rep. 13, 5–6.

Riddle, P.N., 1983. A device for demisting Petri dishes. Lab. Pract. 32, 80.

Rossiello, F., Herbig, U., Longhese, M.P., Fumagalli, M., d'Adda di Fagagna, F., 2014. Irreparable telomeric DNA damage and persistent DDR signalling as a shared causative mechanism of cellular senescence and ageing. Curr. Opin. Genet. Dev. 26, 89–95.

Serrano, M., Blasco, M.A., 2001. Putting the stress on senescence. Curr. Opin. Cell Biol. 13, 748–753.

Shall, S., Stein, W.D., 1979. A mortalization theory for the control of cell proliferation and for the origin of immortal cell lines. J. Theor. Biol. 76, 219–231.

Sherwood, S.W., Rush, D., Ellsworth, J.L., Schimke, R.T., 1988. Defining cellular senescence in IMR-90 cells: a flow cytometric analysis. Proc. Natl. Acad. Sci. 85, 9086–9090.

Shields, R., 1979. Transition probability and the division pattern of WI-38 Cells. Cell Biol. Int. Rep. 3, 659–562.

Smith, J.A., 1977. Application of the theory of transition probability in "ageing" WI 38 cells; similar behaviour of clonogenic cells from early and late passage cultures. Cell Biol. Int. Rep. 1, 283–289.

Smith, J.A., Martin, L., 1973. Do cells cycle? Proc. Natl. Acad. Sci. U. S. A. 70, 1263–1267.

Smith, J.R., Whitney, R.G., 1980. Intraclonal variation in proliferative potential of human diploid fibroblasts: stochastic mechanism for cellular aging. Science 207, 82–84.

Smogorzewska, A., de Lange, T., 2002. Different telomere damage signaling pathways in human and mouse cells. EMBO J. 21, 4338–4348.

Spencer, S.L., Cappell, S.D., Tsai, F.C., Overton, K.W., Wang, C.L., Meyer, T., 2013. The Proliferation-quiescence decision is controlled by a bifurcation in CDK2 activity at mitotic exit. Cell 155, 369–383.

Suram, A., Kaplunov, J., Patel, P.L., Ruan, H., Cerutti, A., Boccardi, V., Fumagalli, M., Di Micco, R., Mirani, N., Gurung, R.L., Hande, M.P., Adda di Fagagna, F., Herbig, U., 2012. Oncogene-induced telomere dysfunction enforces cellular senescence in human cancer precursor lesions. EMBO J. 31, 2839–2851.

Victorelli, S., Passos, J.F., 2017. Telomeres and cell senescence – size matters not. EBioMedicine. https://doi.org/10.1016/j.ebiom.2017.03.027.

von Zglinicki, T., Saretzki, G., Docke, W., Lotze, C., 1995. Mild hyperoxia shortens telomeres and inhibits proliferation of fibroblasts: a model for senescence? Exp. Cell Res. 220, 186–193.

von Zglinicki, T., Pilger, R., Sitte, N., 2000. Accumulation of single-strand breaks is the major cause of telomere shortening in human fibroblasts. Free Radic. Biol. Med. 28, 64–74.

Wright, W.E., Shay, J.W., 2001. Cellular senescence as a tumor-protection mechanism: the essential role of counting. Curr. Opin. Genet. Dev. 11, 98–103.

Wright, W.E., Piatyszek, M.A., Rainey, W.E., Byrd, W., Shay, J.W., 1996. Telomerase activity in human germline and embryonic tissues and cells. Dev. Genet. 18, 173–179.

Wynford-Thomas, D., 2000. Replicative senescence: mechanisms and implications for human cancer. Pathol. Biol. (Paris) 48, 301–307.

Yang, H.W., Chung, M., Kudo, T., Meyer, T., 2017. Competing memories of mitogen and p53 signalling control cell-cycle entry. Nature 549, 404–408.